Bioorthogonal Phosphorogenic Rhenium(I) Polypyridine Sydnone Complexes for Specific Lysosome Labeling

Justin Shum,[a] Pei-Zhi Zhang,[a] Lawrence Cho-Cheung Lee,[a] and Kenneth Kam-Wing Lo*[a, b, c]

Many novel bioorthogonal reactions have been developed for labeling, such as the strain-promoted sydnone-alkyne cycloaddition (SPSAC), but sydnone-based probes with phosphorogenicity (i.e., phosphorescence turn-on upon reaction) have not been investigated to date. Herein, we report the synthesis, characterization, and photophysical properties of rhenium(I) polypyridine complexes containing a sydnone moiety as bioorthogonal phosphorogenic probes. Their reactions with strained alkyne derivatives and the associated photophysical changes were examined. Upon SPSAC with bicyclo[6.1.0]non-4-yn-9-ylmethanol (BCN-OH), the complexes exhibited emission enhancement in the range of 8.8 to 17.3. Importantly, conjugation of the complexes with BCN-modified bovine serum albumin (BCN-BSA) led to the increase in emission enhancement to as high as 38.9 and extended lifetimes in the range of 1.80 to 4.71 μs. Additionally, the bioorthogonal ligation of one of the complexes with a morpholine derivative was shown to induce specific lysosomal labeling in live cells; colocalization studies with LysoTracker Deep Red indicated a Pearson's coefficient of 0.83.

Introduction

Bioorthogonal reactions have been of considerable interest for the design of novel diagnostic and therapeutic agents.[1] These selective chemical reactions can proceed even under complex biological environments without disruption of native processes.[2] Although there has been much success in the development of bioorthogonal handles such as azide,[3] tetrazine,[4] and nitrone,[5] expansion of the bioorthogonal toolbox is still required to allow for greater biological applications and functionality to address crucial medical issues.

Sydnones are mesoionic compounds that are able to undergo thermal 1,3-dipolar cycloadditions with alkynes.[6] Unfortunately, the sydnone cycloaddition with alkynes requires harsh conditions such as high temperatures for long periods of time and would have poor regioselectivity on the resulting pyrazole products.[7] Conversely, the strain-promoted sydnone-alkyne cycloaddition (SPSAC) (Scheme 1) has been shown to readily undergo formation of pyrazole products under ambient conditions.[8] Notably, modification of the sydnone moiety on the position *N*-3 and *C*-4 of the heterocyclic ring offers the capability to tune the reactivity based on the prevalent substituent.[9] Combined with the emission quenching potential of the sydnone functionality, we believe that the SPSAC reaction is an effective tool for the development of luminogenic-based probes for both *in vitro* and *in vivo* imaging. Although various sydnone-based fluorogenic bioorthogonal handles and probes have been synthesized based on organic dyes such as coumarin,[10] napthalimide,[11] and styrylpyridinium,[12] the exploitation of the quenching properties of the sydnone moiety for new phosphorogenic probes has not yet been investigated. Based on the fact that selective bioconjugation has been achieved with transition metal complex-catalyzed organic transformation reactions[13] and with our interest in the use of photofunctional complexes in the development of bioorthogonal handles and imaging probes,[14] we have recently reported new luminescent iridium(III) complexes appended with a sydnone moiety as bioorthogonal handles for cellular imaging.[15] These iridium(III) complexes are always luminescent and display environment-sensitive emission properties. Contrary to this, our new design focuses on bioorthogonal phosphorogenic probes, which utilizes 3-phenyl-4-(4-pyridyl)sydnone (py-syd-ph) as the pyridine ligand for our rhenium(I) polypyridine complexes (Figure 1). Rhenium(I) polypyridine complexes are well known to demonstrate intense, long-lived, and environment-sensitive emission, which renders these complexes as ideal reporters for biological processes and

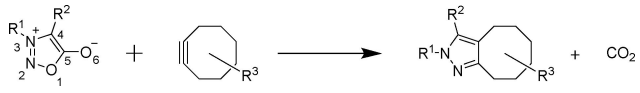

Scheme 1. SPSAC reaction of a sydnone moiety with a strained alkyne leading to the formation of a pyrazole derivative and the subsequent release of a CO_2 molecule.

[a] *J. Shum, Dr. P.-Z. Zhang, L. C.-C. Lee, Prof. K. K.-W. Lo*
Department of Chemistry
City University of Hong Kong
Tat Chee Avenue, Kowloon, Hong Kong (P. R. China)
E-mail: bhkenlo@cityu.edu.hk
[b] *Prof. K. K.-W. Lo*
State Key Laboratory of Terahertz and Millimeter Waves
City University of Hong Kong
Tat Chee Avenue, Kowloon, Hong Kong (P. R. China)
[c] *Prof. K. K.-W. Lo*
Center of Functional Photonics
City University of Hong Kong
Tat Chee Avenue, Kowloon, Hong Kong (P. R. China)

Supporting information for this article is available on the WWW under https://doi.org/10.1002/cplu.202000029

This article is part of a Special Collection on "Fluorescent Biomolecules and their Building Blocks".

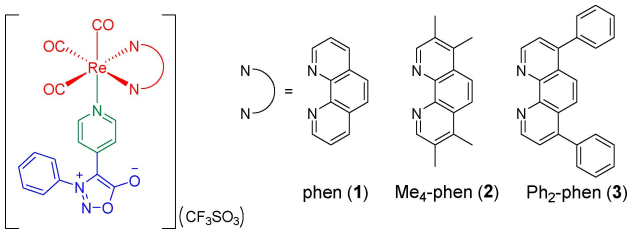

Figure 1. Structures of the rhenium(I) polypyridine sydnone complexes **1**–**3**.

applications. The ligand py-syd-ph was designed due to the π-conjugation between the sydnone unit and the pyridine moiety allowing for efficient emission quenching. Herein, we report the synthesis, characterization, and photophysical properties of three rhenium(I) polypyridine sydnone complexes [Re(N^N)$(CO)_3$(py-syd-ph)](CF_3SO_3) (N^N = 1,10-phenanthroline (phen) (**1**), 3,4,7,8-tetramethyl-1,10-phenanthroline (Me_4-phen) (**2**), 4,7-diphenyl-1,10-phenanthroline (Ph_2-phen) (**3**)) (Figure 1) as new bioorthogonal turn-on reagents for cellular imaging. Synthetic procedures and characterization data can be found in the Supporting Information.

The electronic absorption spectral data of the rhenium(I) complexes are summarized in Table S1 and the electronic absorption spectra of these complexes in CH_2Cl_2 at 298 K are shown in Figure S1 (see the Supporting Information). All the complexes exhibited both intense spin-allowed intraligand (^{1}IL) (π→π*) (N^N and pyridine) absorption bands at ≈ 261–316 nm and metal-to-ligand charge-transfer (^{1}MLCT) (dπ(Re)→π*(N^N)) absorption bands/shoulders at ≈ 320–430 nm. These features are commonly observed in other rhenium(I) polypyridine complexes.[16,17] Upon irradiation, complexes **1** and **3** exhibited extremely weak triplet metal-to-ligand charge transfer (^{3}MLCT) (dπ(Re)→π*(N^N)) emission with a luminescence quantum yield ($\Phi_{em} < 0.0017$, Table 1) which is considerably much lower than those of common rhenium(I) polypyridine complexes.[16,17] The emission of the Me_4-phen complex, which should originate from a ^{3}IL (π→π*) (Me_4-phen) excited state[17] mixed with some ^{3}MLCT (dπ(Re)→π*(Me_4-phen)) character, also displayed a low luminescence quantum yield ($\Phi_{em} < 0.0009$, Table 1). Most likely, these results are due to the polar nature of the sydnone ring providing a highly polar local environment to the complex cores, hence supressing their luminescence quantum yields. Additionally, the π-conjugation of the sydnone moiety towards the rhenium(I) metal center is expected to play a role in the efficient quenching and modulation of the triplet emissive states of the complexes.

The strained alkyne (1*R*,8*S*,9*s*)-bicyclo[6.1.0]non-4-yn-9-ylmethanol (BCN-OH) was used as a substrate for the rhenium(I) complexes to demonstrate the bioorthogonal reactivity of the sydnone moiety. Additionally, of interest, the formation of pyrazole cyclic derivatives from the sydnone core may influence the electronic properties of the conjugated system. The rhenium(I) complexes were incubated with BCN-OH, and interestingly, the resulting pyrazole products (as a mixture of isomers) displayed much stronger emission. Hence, the resulting conjugates were further examined for their phosphorogenic properties and exhibited relatively large emission enhancement (I/I_o) > 8.8, with a hypsochromic shift in the ^{3}MLCT emission maxima of complexes **1** and **3** (Table 2). Complex **2** exhibited the largest enhancement ($I/I_o = 17.3$) in its ^{3}IL emission with a comparable hypsochromic shift.

We were interested whether the turn-on properties and bioorthogonal conjugation of complexes **1**–**3** would be influenced by a change of the reaction partner. Thus, they were then examined for their bioorthogonal labeling properties toward a biological protein model, bovine serum albumin (BSA) conjugated with BCN as an example. The conjugate BCN-BSA was prepared by reaction of BSA with (1*R*,8*S*,9*s*)-bicyclo[6.1.0]non-4-yn-9-ylmethyl *N*-succinimidyl carbonate (BCN-NHS) followed by purification with size-exclusion chromatography. The conjugate and unmodified BSA were incubated with the complexes individually, and the mixtures were then analyzed by SDS-PAGE. As shown from the SDS-PAGE results (Figure 2), BCN-BSA was successfully labeled with the sydnone complexes, which was confirmed by the presence of luminescent bands in the gel. Absence of emission from the unmodified protein samples in their respective lanes indicates the luminescent bands originated from the specific bioorthogonal reaction of the sydnone complexes with the BCN moieties conjugated on the BSA protein. In a separate experiment, the emission enhancement of the rhenium BCN-BSA conjugates was directly measured without purification and varied from 38.9 to 9.6, with extended emission lifetimes (Table 3). This phenomenon is attributed to the increased hydrophobicity and rigidity of the local environment of the complexes after reaction with BCN-BSA which is similar to previously reported studies.[15] Incubation of the complexes with unmodified BSA showed no significant changes in emission enhancement nor emission lifetime (Table 3). The facile reaction of BCN-BSA and the complexes in potassium phosphate buffer solution indicates that the complexes are biocompatible in aqueous media and can only exhibit phosphorogenic response after bioorthogonal

Table 1. Photophysical data of the rhenium(I) polypyridine sydnone complexes in degassed solutions at 298 K.

Complex	Solvent	λ_{em} [nm]	τ [μs]	Φ_{em}
1	CH_2Cl_2	532	0.65	0.0012
	CH_3CN	550	0.58	0.0005
2	CH_2Cl_2	523	1.42	0.0009
	CH_3CN	522	1.30	0.0005
3	CH_2Cl_2	541	1.37	0.0017
	CH_3CN	546	1.25	0.0013

Table 2. Emission maxima and emission enhancement factors (I/I_o) for the rhenium(I) polypyridine sydnone complexes (10 μM) upon reaction with BCN-OH (100 μM) in aerated MeOH at 298 K.

Complex	Complex only λ_{em} [nm]	Complex + BCN-OH λ_{em} [nm]	I/I_o
1	545	535	14.2
2	518	509	17.3
3	557	548	8.8

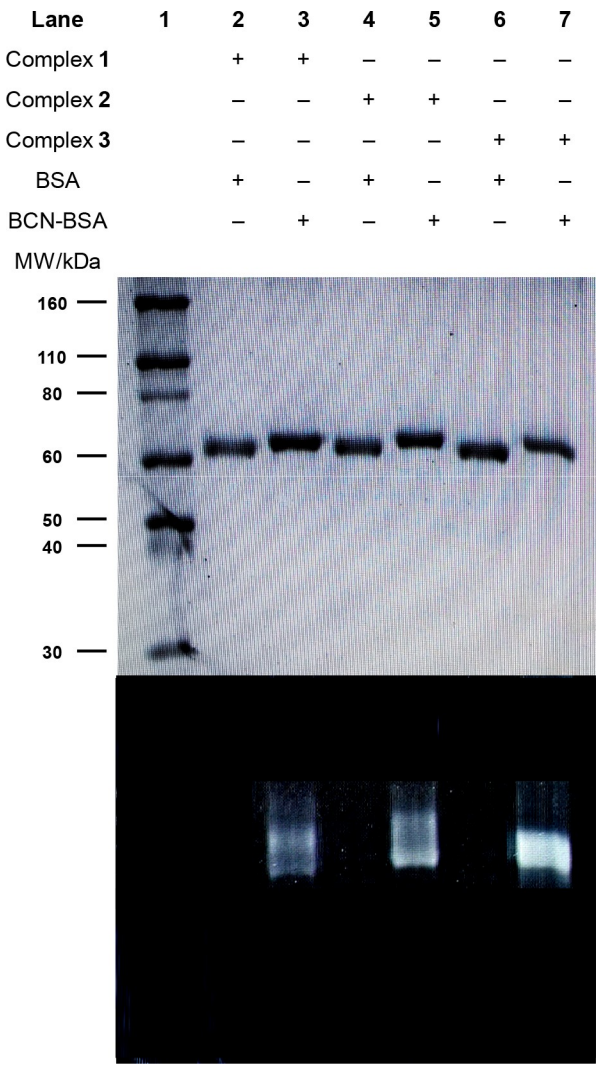

Figure 2. SDS-PAGE analysis of unmodified BSA and BCN-BSA (1 μM) upon incubation with the rhenium(I) polypyridine sydnone complexes (10 μM) in potassium phosphate buffer (50 mM, pH 7.4)/DMSO (9:1, *v/v*) at 298 K. Top: Coomassie Blue Staining; bottom: UV transillumination. Lane 1: protein ladder.

conjugation. The rhenium-to-BSA ratios of all the bioconjugates were determined to be ≈1.0.

The cellular uptake efficiency of the complexes was investigated to examine if the complexes were suitable for cellular imaging. Inductively coupled plasma-mass spectrometry (ICP-MS) measurements indicated the uptake of the complexes followed the order of **3** > **2** > **1**, which is in accordance with the increasing lipophilic character of the ligands: Ph_2-phen > Me_4-phen > phen (Table S2). The cytotoxicity of the complexes toward HeLa cells was determined by the cytotoxicity assay (3-(4,5-dimethylthiazol-2-yl)-2,5-diphenyltetrazolium bromide, MTT) (Figure S3). The half maximal inhibitory concentrations (IC_{50}) of the complexes in order of decreasing cytotoxicity were **3** (4.02 μM) > **2** (25.13 μM) > **1** (> 100 μM), the variation in cytotoxicity of the complexes is due to their differences in uptake efficiency (Table S2). Notably, complex **1** was essentially noncytotoxic (IC_{50} > 100 μM, 20 h; Table S2) under conditions used in the cellular uptake and MTT experiments. The stability of the rhenium(I) complexes in biological media was confirmed by ESI-MS (Figures S4–S6). As a culmination of the noncytotoxic properties and high emission enhancement factor of complex **1**, its potential application as a bioorthogonal phosphorogenic probe for bioimaging of live cells was examined.

Lysosomes are dynamic organelles which are vital in their functions, participating in multiple biological activities such as intracellular digestion, metabolism, and initiation of apoptosis.[18] Various diseases have been linked to defects in lysosome dysfunction,[19] and visualization of these organelles are of upmost importance to improve therapy efficiency. Lysosomal labeling in live cells has been demonstrated by the use of a morpholine molecule.[20] Thus, our strategy was to synthesize a BCN-morpholine (BCN-morph) derivative, by the reaction of BCN-NHS with 4-(2-aminoethyl)morpholine, for targeted lysosomal labeling. We believe that a two-step labeling process will allow greater adaptability, since modification of the targeting moiety on the BCN derivative would allow for cellular localization in other organelles of interest. Subsequent manipulation of the complexes to feature various bioorthogonal groups would enable the tagging of multiple important biomolecules in a single system. The bioorthogonal ligation of BCN-morph with the complexes is illustrated in Scheme 2. Cells were incubated with BCN-morph (100 μM, 1 h), thoroughly washed, incubated with complex **1** (10 μM, 3 h), and thoroughly washed again before imaging. Laser-scanning confocal microscopy (LSCM) revealed that relatively weak emission was observed for conditions involving only complex **1** (10 μM, 3 h) when incubated in HeLa cells, which is in agreement with the strong quenching property of the sydnone unit (Figure 3a). However, incubation of BCN-morph-pretreated cells with complex **1** demonstrated strong punctate staining and much more pronounced emission intensity than untreated cells (Figure 3b), which is due to emission turn-on associated with the successful bioorthogonal ligation of the sydnone complex to BCN-morph. Importantly, co-localization studies indicated the lysosome organelles of the cells were strongly co-stained with the complex and LysoTracker™ Deep Red (Pearson's Coefficient =

Table 3. Photophysical data of the rhenium(I) polypyridine sydnone complexes (10 μM) upon incubation with BCN-BSA (1 μM) in aerated potassium phosphate buffer (50 mM, pH 7.4)/DMSO (9:1, *v/v*) at 298 K.

Complex	Complex only		Complex + BSA			Complex + BCN-BSA		
	λ_{em} [nm]	τ [μs]	λ_{em} [nm]	I/I_o	τ [μs]	λ_{em} [nm]	I/I_o	τ [μs]
1	547	0.56	556	1.1	0.56	529	26.8	1.80
2	526	1.30	529	1.3	1.26	513	38.9	4.71
3	566	0.98	568	1.1	0.96	554	9.6	1.87

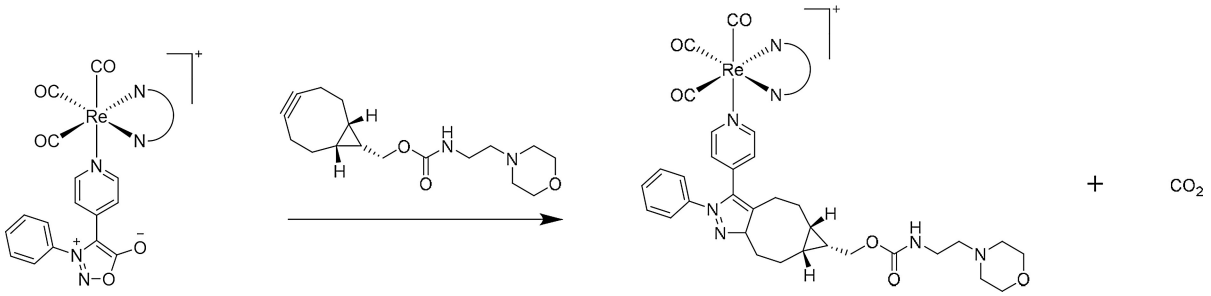

Scheme 2. Bioorthogonal ligation of BCN-morph with complexes **1**–**3**.

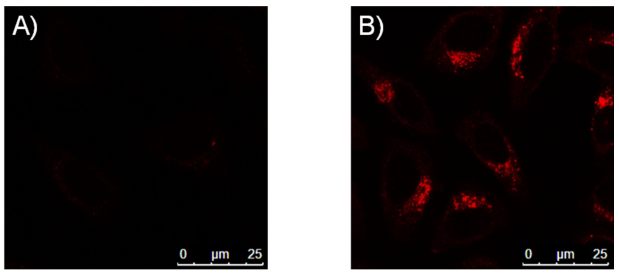

Figure 3. LSCM images of live HeLa cells incubated with complex **1** (10 µM, 3 h, λ_{ex} = 405 nm) without (A) or with (B) pretreatment with BCN-morph (100 µM, 1 h) at 37 °C.

0.83) (Figure 4). Subsequent co-localization studies with MitoTracker™ Deep Red FM demonstrated noticeably very weak co-staining of the mitochondria (Pearson's Coefficient = 0.38) (Figure 5), highlighting the specificity of complex **1** toward the lysosome organelles. These results suggest that the complex can be used in effective lysosomal staining in live HeLa cells.

In conclusion, we synthesized novel phosphorogenic rhenium(I) polypyridine sydnone complexes for further expansion of the bioorthogonal toolbox. These complexes demonstrated emission turn-on capabilities after SPSAC with BCN-OH. Further studies of the bioorthogonal ligation on BCN-BSA also indicated emission enhancement. As a result of the essentially non-cytotoxic properties and emission enhancement capabilities of

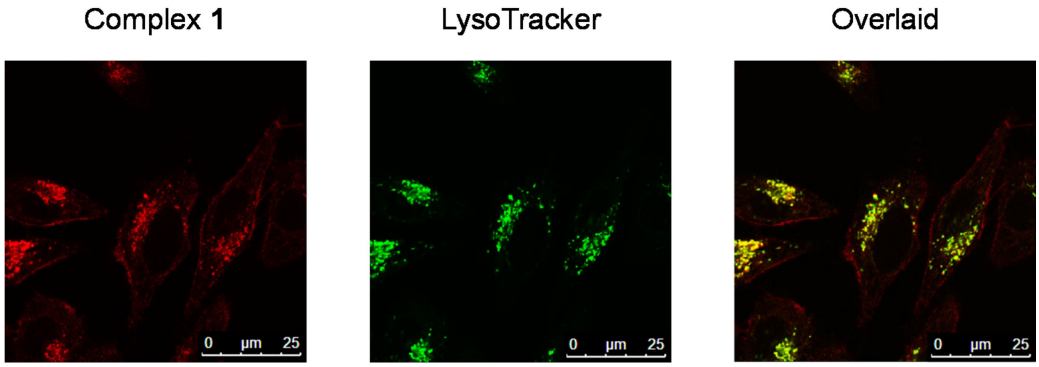

Figure 4. LCSM images of live HeLa cells pretreated with BCN-morph (100 µM, 1 h) and incubated with complex **1** (10 µM, 3 h, λ_{ex} = 405 nm) and LysoTracker™ Deep Red (100 nM, 30 min, λ_{ex} = 635 nm) at 37 °C.

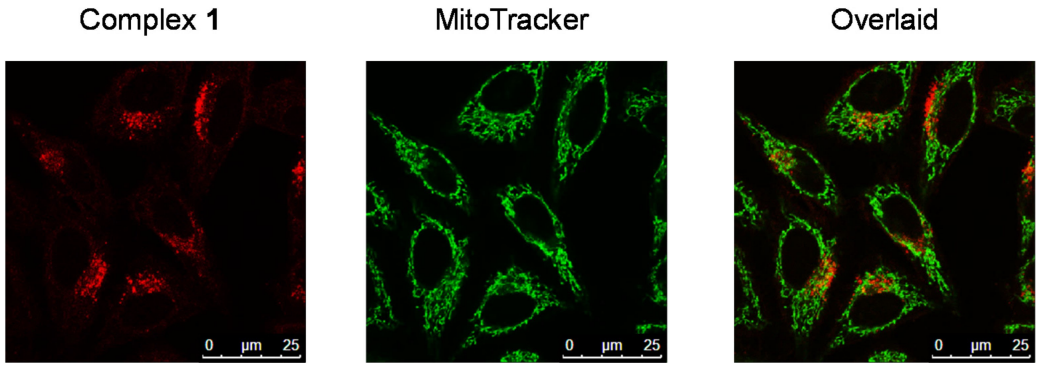

Figure 5. LCSM images of live HeLa cells pretreated with BCN-morph (100 µM, 1 h) and incubated with complex **1** (10 µM, 3 h, λ_{ex} = 405 nm) and MitoTracker™ Deep Red (100 nM, 30 min, λ_{ex} = 635 nm) at 37 °C.

complex **1**, it was utilized for bioimaging studies in live HeLa cells. Co-localization studies demonstrated strong lysosomal labeling, indicative of the successful bioorthogonal ligation of BCN-morph and the complex. These results indicate that the rhenium(I) polypyridine sydnone complexes are promising as novel bioorthogonal phosphorogenic labeling reagents for biological applications.

Acknowledgements

We thank the Hong Kong Research Grants Council (Project No. CityU 11300019, CityU 11300318, CityU 11300017, and T42-103/16-N) and the Hong Kong Research Grants Council, National Natural Science Foundation of China (Project No. N_CityU113/15) for financial support. J.S. acknowledges the receipt of a Postgraduate Studentship administered by City University of Hong Kong. L.C.-C.L. acknowledges the receipt of a Postgraduate Studentship, a Research Tuition Scholarship, and an Outstanding Academic Performance Award administrated by City University of Hong Kong.

Conflict of Interest

The authors declare no conflict of interest.

Keywords: bioorthogonal reactions · imaging agents · phosphorogenic probes · rhenium · sydnones

[1] a) P. Shieh, C. R. Bertozzi, *Org. Biomol. Chem.* **2014**, *12*, 9307–9320; b) R. K. V. Lim, Q. Lin, *Chem. Commun.* **2010**, *46*, 1589–1600; c) C. P. Ramil, Q. Lin, *Chem. Commun.* **2013**, *49*, 11007–11022.
[2] E. M. Sletten, C. R. Bertozzi, *Angew. Chem. Int. Ed.* **2009**, *48*, 6974–6998; *Angew. Chem.* **2009**, *121*, 7108–7133.
[3] a) V. V. Rostovtsev, L. G. Green, V. V. Fokin, K. B. Sharpless, *Angew. Chem. Int. Ed.* **2002**, *41*, 2596–2599; *Angew. Chem.* **2002**, *114*, 2708–2711; b) C. W. Tornøe, C. Christensen, M. Meldal, *J. Org. Chem.* **2002**, *67*, 3057–3064.
[4] a) J. C. T. Carlson, L. G. Meimetis, S. A. Hilderbrand, R. Weissleder, *Angew. Chem. Int. Ed.* **2013**, *52*, 6917–6920; *Angew. Chem.* **2013**, *125*, 7055–7058; b) J. Šečkutė, N. K. Devaraj, *Curr. Opin. Chem. Biol.* **2013**, *17*, 761–767; c) A. W.-T. Choi, K. K.-S. Tso, V. M.-W. Yim, H.-W. Liu, K. K.-W. Lo, *Chem. Commun.* **2015**, *51*, 3442–3445; d) T. S.-M. Tang, H.-W. Liu, K. K.-W. Lo, *Chem. Commun.* **2017**, *53*, 3299–3302.
[5] a) X. Ning, R. P. Temmig, J. Dommerholt, J. Guo, D. B. Ania, M. F. Debets, M. A. Wolfert, G.-J. Boons, F. L. van Delft, *Angew. Chem. Int. Ed.* **2010**, *49*, 3065–3068; *Angew. Chem.* **2010**, *122*, 3129–3132; b) L. C.-C. Lee, J. C.-W. Lau, H.-W. Liu, K. K.-W. Lo, *Angew. Chem. Int. Ed.* **2016**, *55*, 1046–1049; *Angew. Chem.* **2016**, *128*, 1058–1061; c) T. S.-M. Tang, H.-W. Liu, K. K.-W. Lo, *Chem. Eur. J.* **2016**, *22*, 9649–9659.
[6] E. Decuypère, L. Plougastel, D. Audisio, F. Taran, *Chem. Commun.* **2017**, *53*, 11515–11527.
[7] a) K. N. Houk, J. Sims, R. E. Duke, R. W. Strozier, J. K. George, *J. Am. Chem. Soc.* **1973**, *95*, 7287–7301; b) K. N. Houk, J. Sims, C. R. Watts, L. J. Luskus, *J. Am. Chem. Soc.* **1973**, *95*, 7301–7315.
[8] a) E. Yen-Pon, P. A. Champagne, L. Plougastel, S. Gabillet, P. Thuéry, M. Johnson, G. Muller, G. Pieters, F. Taran, K. N. Houk, D. Audisio, *J. Am. Chem. Soc.* **2019**, *141*, 1435–1440; b) S. Kolodych, E. Rasolofonjatovo, M. Chaumontet, M.-C. Nevers, C. Créminon, F. Taran, *Angew. Chem. Int. Ed.* **2013**, *52*, 12056–12060; *Angew. Chem.* **2013**, *125*, 12278–12282; c) S. Wallace, J. W. Chin, *Chem. Sci.* **2014**, *5*, 1742–1744.
[9] a) L. Plougastel, O. Koniev, S. Specklin, E. Decuypère, C. Créminon, D.-A. Buisson, A. Wagner, S. Kolodych, F. Taran, *Chem. Commun.* **2014**, *50*, 9376–9378; b) H. Liu, D. Audisio, L. Plougastel, E. Decuypère, D.-A. Buisson, O. Koniev, S. Kolodych, A. Wagner, M. Elhabiri, A. Kryzczmonik, S. Forsback, O. Solin, V. Gouverneur, F. Taran, *Angew. Chem. Int. Ed.* **2016**, *55*, 12073–12077; *Angew. Chem.* **2016**, *128*, 12252–12256.
[10] a) C. Favre, F. Friscourt, *Org. Lett.* **2018**, *20*, 4213–4217; b) E. Decuypè, M. Riomet, A. Sallustrau, S. Bregant, R. Thai, G. Pieters, G. Clavier, D. Audisio, F. Taran, *Chem. Commun.* **2018**, *54*, 10758–10761.
[11] Z. Shao, C. Zhang, X. Zhu, Y. Wang, W. Xu, Y. Chen, X. Wang, H. Zhu, Y. Liang, *Chin. Chem. Lett.* **2019**, *30*, 2169–2172.
[12] L. Plougastel, M. R. Pattanayak, M. Riomet, S. Bregant, A. Sallustrau, M. Nothisen, A. Wagner, D. Audisio, F. Taran, *Chem. Commun.* **2019**, *55*, 4582–4585.
[13] a) M. N. Wenzel, R. Bonsignore, S. R. Thomas, D. Bourissou, G. Barone, A. Casini, *Chem. Eur. J.* **2019**, *25*, 7628–7634; b) A. Schimdt, V. Molano, M. Hollering, A. Pöthig, A. Casini, *Chem. Eur. J.* **2016**, *22*, 2253–2256.
[14] K. K.-W. Lo, *Acc. Chem. Res.* **2020**, *53*, 32–44.
[15] L. C.-C. Lee, H. M.-H. Cheung, H.-W. Liu, K. K.-W. Lo, *Chem. Eur. J.* **2018**, *24*, 14064–14068.
[16] a) L. Wallace, D. P. Rillema, *Inorg. Chem.* **1993**, *32*, 3836–3843; b) A. M.-H. Yip, J. Shum, H.-W. Liu, H. Zhou, M. Jia, N. Niu, Y. Li, C. Yu, K. K.-W. Lo, *Chem. Eur. J.* **2019**, *25*, 8970–8974; c) A. W.-T. Choi, H.-W. Liu, K. K.-W. Lo, *J. Inorg. Biochem.* **2015**, *148*, 2–10; d) A. W.-T. Choi, V. M.-W. Yim, H.-W. Liu, K. K.-W. Lo, *Chem. Eur. J.* **2014**, *20*, 9633–9642.
[17] a) L. Sacksteder, M. Lee, J. N. Demas, B. A. DeGraff, *J. Am. Chem. Soc.* **1993**, *115*, 8230—8238; b) L. Wallace, D. C. Jackman, D. P. Rillema, J. W. Merket, *Inorg. Chem.* **1995**, *34*, 5210–5214.
[18] a) U. Repnik, V. Stoka, V. Turk, B. Turk, *Biochim. Biophys. Acta.* **2012**, *1824*, 22–33; b) M. E. Guicciardi, M. Leist, G. J. Gores, *Oncogene* **2004**, *23*, 2881–2890.
[19] a) T. M. Cox, M. B. Cachón-González, *J. Pathol.* **2011**, *226*, 241–254; b) T. Pan, S. Kondo, W. Le, J. Jankovic, *Brain* **2008**, *131*, 1969–1978.
[20] a) J. Zhang, M. Yang, W. Mazi, K. Adhikari, M. Fang, L. Valenzano, A. Tiwari, F.-T. Luo, H. Liu, *ACS Sens.* **2016**, *1*, 158–165; b) C. W. T. Leung, Z. Wang, E. Zhao, Y. Hong, S. Chen, R. T. K. Kwok, A. C. S. Leung, R. Wen, B. Li, J. W. Y. Lam, B. Z. Tang, *Adv. Healthcare Mater.* **2016**, *5*, 427–431; c) Q. Wan, S. Chen, W. Shi, L. Li, H. Ma, *Angew. Chem. Int. Ed.* **2014**, *53*, 10916–10920; *Angew. Chem.* **2014**, *126*, 11096–11100.

Manuscript received: January 20, 2020
Revised manuscript received: March 4, 2020
Accepted manuscript online: March 5, 2020